The Astrophysical Journal, 829:99 (8pp), 2016 October 1 doi:10.3847/0004-637X/829/2/99

REVISITING THE LYMAN CONTINUUM ESCAPE CRISIS: PREDICTIONS FOR $z > 6$ FROM LOCAL GALAXIES

Andreas L. Faisst
Infrared Processing and Analysis Center, California Institute of Technology, Pasadena, CA 91125, USA, afaisst@ipac.caltech.edu, Twitter:@astrofaisst
Received 2016 May 20; revised 2016 June 29; accepted 2016 July 19; published 2016 September 27

ABSTRACT

The intrinsic escape fraction of ionizing Lyman continuum photons ($f_{\rm esc}$) is crucial to understanding whether galaxies are capable of reionizing the neutral hydrogen in the early universe at $z > 6$. Unfortunately, it is not possible to access $f_{\rm esc}$ at $z > 4$ with direct observations, and the handful of measurements from low-redshift galaxies consistently find $f_{\rm esc} < 10\%$, while at least $f_{\rm esc} \sim 10\%$ is necessary for galaxies to dominate reionization. Here, we present the first empirical prediction of $f_{\rm esc}$ at $z > 6$ by combining the (sparsely populated) relation between [O III]/[O II] and $f_{\rm esc}$ with the redshift evolution of [O III]/[O II] as predicted from local high-z analogs selected by their Hα equivalent width. We find $f_{\rm esc} = 5.7^{+8.3}_{-3.3}\%$ at $z = 6$ and $f_{\rm esc} = 10.4^{+15.5}_{-6.3}\%$ at $z = 9$ for galaxies with $\log(M/M_{\odot}) \sim 9.0$ (errors given as 1σ). However, there is a negative correlation with stellar mass and we find up to 50% larger $f_{\rm esc}$ per 0.5 dex decrease in stellar mass. The population-averaged escape fraction increases according to $f_{\rm esc} = f_{\rm esc,0}\,((1+z)/3)^{\alpha}$, with $f_{\rm esc,0} = (2.3 \pm 0.05)\%$ and $\alpha = 1.17 \pm 0.02$ at $z > 2$ for $\log(M/M_{\odot}) \sim 9.0$. With our empirical prediction of $f_{\rm esc}$ (thus fixing an important, previously unknown variable) and further reasonable assumptions on clumping factor and the production efficiency of Lyman continuum photons, we conclude that the average population of galaxies is just capable of reionizing the universe by $z \sim 6$.

Key words: galaxies: evolution – galaxies: high-redshift – galaxies: ISM

1. INTRODUCTION

A major phase transition in the early universe takes place during the Epoch of Reionization (EoR), in which hydrogen in the intergalactic medium (IGM) is transformed from a neutral to an ionized state. The EoR is closely connected to the formation of the first galaxies, and thus the study of its evolution in time and space is important for understanding galaxy formation in the early universe.

The study of absorption due to intervening neutral hydrogen in the IGM in ultraviolet (UV) spectra of quasars allows us to pinpoint the end of the EoR (i.e., the time when the universe is fully ionized) to $z \sim 6$ (Fan et al. 2006; McGreer et al. 2011; Mortlock et al. 2011). Furthermore, the rapid decrease in the fraction of star-forming high-redshift galaxies with Lyα emission at $z > 6$ suggests that the universe became ionized very quickly on timescales of only a few hundred million years between $z \sim 6$ and $z \sim 10$ (e.g., Stark et al. 2010; Ono et al. 2012; Schenker et al. 2013; Faisst et al. 2014; Matthee et al. 2014; Robertson et al. 2015). In addition to these direct observations, the temperature fluctuations in the cosmic microwave background (CMB) allow the measurement of the integrated density of free electrons from $z = 0$, through the EoR, to $z \sim 1100$ when the CMB emerged. Recent measurements suggest $\tau_e = 0.055 \pm 0.009$ and constrain the end of the EoR to $7.8 \lesssim z_{\rm ion} \lesssim 8.8$, assuming an immediate ionization of hydrogen (Planck Collaboration et al. 2016).

Although such observations are able to reveal the time frame of the EoR, we are mostly tripping in the dark about the origin of the dominant ionizing sources. Quasars and star-forming galaxies are currently the competing players for providing energetic photons to ionize hydrogen at $z > 6$. However, because of the suggested sharp decline in the number density of quasars with increasing redshift at $z > 6$, they likely do not dominate the budget of radiation needed to ionize hydrogen[1] (e.g., Masters et al. 2012; Palanque-Delabrouille et al. 2013). On the other hand, the overall number density of UV-emitting, faint star-forming galaxies has dropped only slightly in the period $6 < z < 9$ (Schenker et al. 2013; Tacchella et al. 2013; Oesch et al. 2014; Bouwens et al. 2015b; Mason et al. 2015). Furthermore, studies of faint, lensed galaxies show the continuation of the UV luminosity function (LF) to very faint magnitudes (Alavi et al. 2014; Livermore et al. 2016), thus providing an important number of galaxies needed for reionization.

The redshift evolution of the volume fraction of ionized hydrogen ($Q_{\rm H\,II}$) and the integral of the electron scattering optical depth ($\tau_{\rm el}(z)$, the integrated density of free electrons to redshift z) allow us to test whether galaxies are actually capable of reionizing the universe (e.g., Finkelstein et al. 2012; Kuhlen & Faucher-Giguère 2012; Bouwens et al. 2015a; Robertson et al. 2015; Price et al. 2016). Unfortunately, the determination of $Q_{\rm H\,II}(z)$ and $\tau_{\rm el}(z)$ involves several properties of galaxies and their environment that cannot be measured directly or have to be accessed via cosmological simulations. In detail, these dependences are the faint-end slope of the UV LF and its cutoff magnitude ($M_{\rm UV,lim}$), the clumping of hydrogen in the IGM (C), the photon production efficiency ($\xi_{\rm ion}$) of the Lyman continuum (LyC), and the intrinsic escape fraction of ionizing LyC photons ($f_{\rm esc}$). We have a good handle on $M_{\rm UV,lim}$ from lensing (see above), and good estimates of $\xi_{\rm ion}$ at $z \sim 5$ (e.g., Bouwens et al. 2015c)[2], and can provide a reasonable range in C from cosmological simulations (e.g., Finlator et al. 2012). In

[1] However, they contribute to the reionization of helium at $z \sim 3$ (see also Madau & Haardt 2015).

[2] Note that this measurement depends on the assumed stellar populations. Specifically, the inclusion of binary stellar populations may lead to significantly higher $\xi_{\rm ion}$ (Ma et al. 2016; Stanway et al. 2016; Steidel et al. 2016; Wilkins et al. 2016).

contrast, f_{esc} is puzzling, and unfortunately it directly affects $Q_{H\,II}$ and τ_{el} and therefore our picture of galaxies during reionization.

With only f_{esc} as a free parameter, different studies suggest that $f_{esc} = 10\%$–20% at $z > 6$ is necessary for galaxies to fully ionize the universe (Bolton & Haehnelt 2007b; Finkelstein et al. 2012; Kuhlen & Faucher-Giguère 2012; Bouwens et al. 2015a, 2015c; Mitra et al. 2015; Robertson et al. 2015; Khaire et al. 2016; Price et al. 2016). Simulations do not agree on f_{esc} at high redshifts and find either very high (e.g., Sharma et al. 2016) or very low values (e.g., Gnedin et al. 2008; Ma et al. 2015). Furthermore, they predict a strong dependence on the mass of dark matter halos and star formation (e.g., Wise & Cen 2009; Razoumov & Sommer-Larsen 2010). Direct observational constraints on f_{esc} in the EoR are not possible because of the increasing opacity of the IGM to LyC photons at $z > 4$ (e.g., Madau 1995; Inoue et al. 2014). Except for one strong LyC emitter at $z = 3.2$ with $f_{esc} > 50\%$ (de Barros et al. 2016; Vanzella et al. 2016b), the handful of confirmed LyC emitters at $z < 3$ all show consistently $f_{esc} \lesssim 8\%$ (Steidel et al. 2001; Leitet et al. 2013; Borthakur et al. 2014; Cooke et al. 2014; Siana et al. 2015; Izotov et al. 2016a, 2016b; Leitherer et al. 2016; Smith et al. 2016). The numerous non-detections listed in the literature show upper limits of $f_{esc} \sim 2\%$–5% over large ranges of redshift (Vanzella et al. 2010; Sandberg et al. 2015; Grazian et al. 2016; Guaita et al. 2016; Rutkowski et al. 2016; Vasei et al. 2016). If galaxies are responsible for ionizing the universe at $z > 6$, then clearly their population-averaged LyC escape fraction needs to increase substantially with redshift by at least a factor of two (see also Inoue et al. 2006). What methods can we use to access f_{esc} observationally in the EoR? Radiative transfer models suggest a correlation between the ratio [O III]/[O II] and f_{esc} in density-bound H II regions (e.g., Nakajima & Ouchi 2014), and a handful of recent observational studies verify this positive correlation (de Barros et al. 2016; Izotov et al. 2016a, 2016b; Vanzella et al. 2016a, 2016b). The increased [O III]/Hβ ratios found in $z > 5$ galaxies (e.g., Stanway et al. 2014; Roberts-Borsani et al. 2015; Faisst et al. 2016a) hint toward an increasing [O III]/[O II] ratio for the global population of galaxies at high redshifts and therefore could be the smoking gun for a strong evolution in $f_{esc}(z)$. Currently, the [O II] line cannot be measured spectroscopically at $z > 4$, and the use of broad-band photometry to determine [O II] line strengths is degenerate with the 4000 Å Balmer break, which is a strong function of age and other galaxy parameters. However, local analogs of high-redshift galaxies can be used to probe the physical properties of these galaxies.

This paper aims to provide the first observationally based prediction of f_{esc} in galaxies at $z > 6$. To this end, we select local high-z analogs (LHAs) by their Hα emission (see Faisst et al. 2016a). We use these to predict the [O III]/[O II] ratios of high-redshift galaxies and, with an empirical correlation between [O III]/[O II] and f_{esc}, ultimately the redshift evolution of f_{esc} (Section 2). With our prediction of f_{esc} we then derive $Q_{H\,II}(z)$ and $\tau_{el}(z)$ and comment on the capability of galaxies to reionize the early universe (Section 3). Throughout this work we adopt a flat cosmology with $\Omega_{\Lambda,0} = 0.7$, $\Omega_{m,0} = 0.3$, and $h = 0.7$. All stellar masses are scaled to a Chabrier (2003) initial mass function.

2. PREDICTING f_{esc} AT HIGH REDSHIFTS

2.1. Locals as Analogs for High-redshift Galaxies

The resemblance of the physical properties of high-redshift galaxies and subsets of galaxies at low ($z < 1$) or local ($z \sim 0$) redshifts has been known for almost a decade and is a subject of study in the very recent literature (Cardamone et al. 2009; Stanway et al. 2014; Bian et al. 2016; Erb et al. 2016; Faisst et al. 2016a; Greis et al. 2016; Masters et al. 2016). Some of the most famous representatives of low-redshift high-z analogs are the "Green Peas" at $z \sim 0.2$ (Cardamone et al. 2009) or the ultra-strong emission line galaxies (USELs) at $z \sim 0.8$ (Hu et al. 2009). In any case, the LHAs are characterized by an increased surface density of star formation rate (SFR) and Hα equivalent width (EW)[3] compared to the average local galaxy population (e.g., Masters et al. 2016). In particular, Faisst et al. (2016a) measure the [O III]/Hβ line ratios of average $z \sim 5.5$ galaxies via the *Spitzer* color excess and verify a good agreement with LHAs selected by EW(Hα) > 300 Å. This first-order verification motivates the use of LHAs selected by Hα EW to predict spectroscopic properties of high-redshift galaxies in the EoR. Here, we use a sample of more than 100,000 local ($z < 0.1$) galaxies drawn from the Sloan Digital Sky Survey (SDSS, York et al. 2000) DR12 release (Alam et al. 2015) using the SDSS query tool.[4] The galaxies are selected to have signal-to-noise ratio S/N > 5 in all the important optical emission lines ([O II], [O III], Hα, Hβ, and [N II]), and no component from active galactic nuclei. We select LHAs for galaxies at a redshift z by selecting SDSS galaxies with $\mathrm{EW(H}\alpha)|_{SDSS} = \mathrm{EW(H}\alpha)(z) \pm \Delta(z)$, using the relation for EW(Hα)(z) presented in Faisst et al. (2016a) including the 1σ confidence interval (Δ) in EW at a given z. The relation between EW(Hα) and redshift has been measured using various spectroscopic surveys at $z \sim 0$–3 (e.g., Erb et al. 2006; Steidel et al. 2014; Silverman et al. 2015; Sobral et al. 2015) as well as up to $z \sim 6$ (e.g., Faisst et al. 2016a) using the excess in *Spitzer* [3.6 μm] – [4.5 μm] colors for a large sample of galaxies with spectroscopic redshift determinations as part of the Cosmic Evolution Survey (Scoville et al. 2007). For further details of the derivation of this relation, we refer the reader to Faisst et al. (2016a). Here we give the parameterization of this relation as

$$\mathrm{EW(H}\alpha)(z) = \begin{cases} 20^{+15}_{-8} \times (1+z)^{1.87}, & z < 2.2 \\ 37^{+51}_{-7} \times (1+z)^{1.30}, & z \geqslant 2.2 \end{cases} \quad (1)$$

The error is given in the normalization and accounts for the physical scatter as well as the uncertainties of the measurements at low and high redshift. These uncertainties are propagated through this analysis and are included in the following results. We stress that, despite the obvious similarities of LHAs and intermediate galaxies ($z \sim 2$, see also Figure 1), the use of LHAs to infer the properties of very high-redshift galaxies has not yet been fully verified. The following results therefore depend strongly on the assumption that strong Hα-emitting local galaxies (equivalent to high specific SFR) are indeed similar to actual high-z galaxies and that the ISM properties do not depend greatly on the environment in which a galaxy was formed. This does not have to be the case, since the cradles of formation for very high-z galaxies are surely

[3] Note that EW(Hα) is proportional to the specific SFR of a galaxy.

[4] http://skyserver.sdss.org/dr12/en/tools/search/sql.aspx

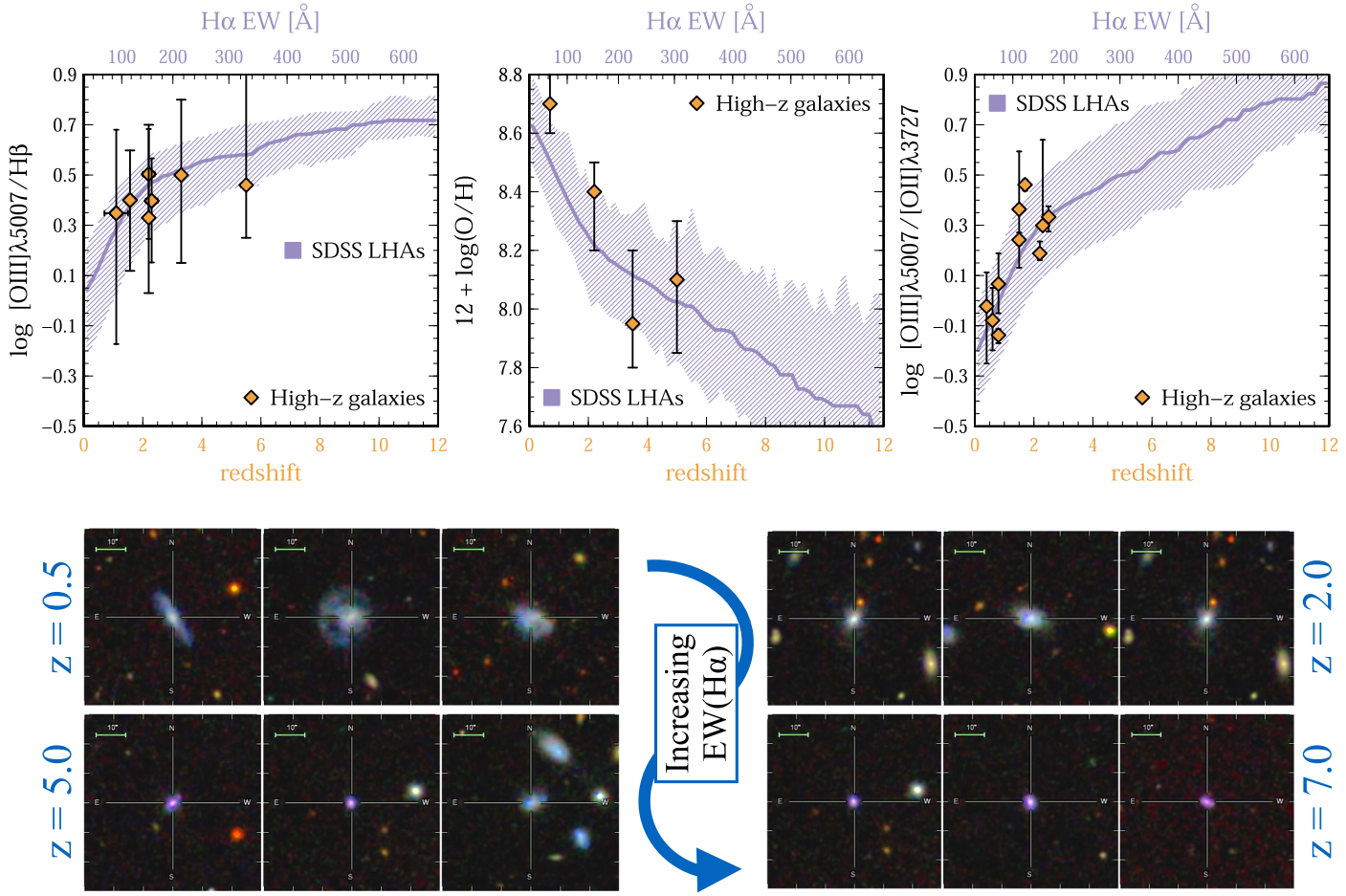

Figure 1. Top: the predicted redshift evolution of [O III]/Hβ (left), metallicity (middle), and [O III]/[O II] (right) from LHAs selected by Hα EW in SDSS. The purple hatched band shows these properties as a function of EW(Hα) (upper x-axis) for the local SDSS galaxies. The orange symbols show these properties for intermediate- and high-redshift galaxies (see text for references) as a function of redshift (bottom x-axis). This comparison motivates the use of local galaxies selected by EW(Hα)as analogs for high-redshift galaxies. The connection between EW(Hα) and redshift is as given in Equation (1) (see also Faisst et al. 2016a). Bottom: SDSS color composites of three randomly picked representatives of LHAs for four different Hα EWs, mimicking four different redshifts ($z = 0.5$, 2.0, 5.0, 7.0 from left to right and top to bottom; stamps are $60'' \times 60''$ in size). The LHAs show similar morphology to observed high-redshift galaxies.

different (more dense, more galaxy interactions) to those of local galaxies. Ultimately, the *James Webb Space Telescope* (*JWST*) will be able to test these assumptions further and will provide a clearer picture.

2.2. Predicted Emission Line Ratios of High-z Galaxies

The top panels of Figure 1 show the dependence of the spectroscopic properties of the local SDSS galaxies on EW(Hα) for galaxies with $8.5 < \log(M/M_\odot) < 9.5$ with a median of $\log(M/M_\odot) \sim 9.0$ (similar to the galaxies observed at high redshift). The dependence of these relations on stellar mass is discussed in Section 2.4. We show the dependence of [O III]/Hβ ratio (left), gas-phase metallicity[5] (middle), and [O III]/[O II] ratio (right) on EW(Hα) (top x-axis), with the median shown as a purple line and the 1σ scatter visualized by the purple hatched band. Together with Equation (1) and the assumption that these galaxies are high-z galaxy analogs, this can be interpreted as a redshift evolution of these quantities (bottom x-axis), which allows us to predict the spectroscopic properties of galaxies at higher redshifts. The open orange symbols show the measurement of the three quantities for actual galaxies at high redshift (from either spectroscopy or *Spitzer* color excess at $z > 4$) from the literature (for [O III]/Hβ: Colbert et al. 2013; Steidel et al. 2014; Silverman et al. 2015; Sanders et al. 2016; for metallicity: Maiolino et al. 2008; Faisst et al. 2016b; for [O III]/[O II]: Rigby et al. 2011; Le Fèvre et al. 2013; de los Reyes et al. 2015; Hayashi et al. 2015; Khostovan et al. 2016). All in all, there is a good agreement in all the shown spectral properties of LHAs selected purely by EW(Hα) and actual high-redshift galaxies up to $z \sim 5$, where current measurements of [O II], [O III], and Hβ are possible. This suggests that the Hα EW (closely related to the specific SFR) is strongly correlated with the conditions of the ISM in these galaxies, or, vice versa, that the ISM of galaxies with strong Hα emission is very similar at all redshifts at least up to $z \sim 5$. Under the assumption of EW(Hα) being the main diagnostic of the spectral properties of galaxies, we use it as the quantity for the selection of local galaxies to predict the spectral properties of galaxies at $z > 5$ where currently no such measurements are possible. As mentioned in Section 2.1, this assumption has yet to be tested by the next generation of telescopes such as *JWST*.

From the LHAs we infer *average* [O III]/Hβ ratios of ~4–5 and [O III]/[O II] ratios larger than 3–4 at $6 < z < 8$. The gas-phase metallicities of $z > 6$ galaxies are predicted to be $12 + \log(\mathrm{O/H}) < 8.0$ on average, but with a substantial

[5] Metallicities are shown in the calibration of Maiolino et al. (2008).

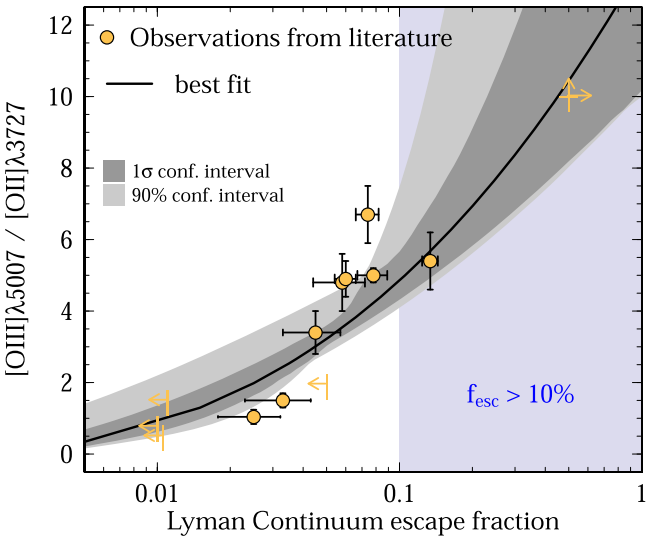

Figure 2. Observed correlation between [O III]/[O II] ratio and f_{esc} from a compilation of literature data with limits shown by arrows. The black line shows the best-fit median relation with an envelope of the 1σ and 90% confidence interval. The analytical parameterization is given in Equation (2). The blue shaded area shows $f_{esc} > 10\%$, needed for galaxies at $z > 6$ to reionize the universe.

scatter leading to values above 8.0 for some galaxies. Such large scatter is consistent with measurements of metallicity in $z \sim 5$ galaxies based on rest-UV absorption features and is expected from the different evolutionary stages and dust attenuation as well as gas inflows in these systems (e.g., Faisst et al. 2016b).

Finally, the bottom panels of Figure 1 show the morphological resemblance of our LHAs to high-redshift galaxies. With increasing EW(Hα) (and therefore corresponding redshift), the LHAs become more compact and blue and show clumps in UV light as seen in high-redshift galaxies at $z = 2$–4 (e.g., Förster Schreiber et al. 2011; Hemmati et al. 2015).

2.3. Correlation between [O III]/[O II] and f_{esc}

The absorption of Lyman continuum photons in the IGM increases quickly by a factor of 100 or more close to $z \sim 4$ (e.g., Inoue et al. 2014). The direct measurement of the galaxy intrinsic f_{esc} at redshifts greater than this is therefore not possible. However, its theoretically and observationally motivated connection with the [O III]/[O II] ratio may allow us to make predictions of f_{esc} for distant galaxies.

Commonly, f_{esc} is measured in local galaxies from spectra or at intermediate redshifts by the detection of excess flux in narrow-band filters at rest-frame $\lambda < 900$ Å. As summarized in Section 1, the detection of Lyman continuum photons turns out to be difficult, and current searches are mostly ending in non-detections. With the recent addition of Lyman continuum detections in mostly local galaxies, the positive correlation between f_{esc} and the [O III]/[O II] ratio became observationally clear. The [O III]/[O II] ratio is a measure of the ionization parameter in galaxies, which correlates with the star formation density and thus the production of UV photons. A positive correlation is expected from radiative transfer simulations and is physically motivated by density-bound H II regions and stronger radiation fields that prevail in high-redshift galaxies. In such environments, an increase in [O III] flux, at a roughly constant [O II] emission, is expected in connection with a large number of escaping ionizing photons and therefore high f_{esc} (e.g., Nakajima & Ouchi 2014). In Figure 2, we show eight detections of f_{esc} and four upper limits, each of them with reliable spectroscopic measurements of [O II] and [O III] (Leitet et al. 2013; Borthakur et al. 2014; Izotov et al. 2016a, 2016b; Leitherer et al. 2016; Vanzella et al. 2016b). The limit at [O III]/[O II] > 10 (estimated from only a spectroscopic detection of [O III]) and $f_{esc} > 50\%$ shows the recent detection at $z = 3.2$ (de Barros et al. 2016; Vanzella et al. 2016b). The positive correlation between f_{esc} and [O III]/[O II] ratio is evident, although mostly driven by the limit at large f_{esc}. It should therefore be used with caution and its uncertainty must be included in the following analysis. We describe this relation with the analytical form

$$[\mathrm{O\,III}]/[\mathrm{O\,II}] = \phi + (\phi + a)^b + a, \quad (2)$$

and use the substitution $\phi = \log(f_{esc})$. The best fit ($a = 2.60^{+0.09}_{-0.09}$ and $b = 2.52^{+0.83}_{-0.16}$) is shown as a black line. The gray band shows the 1σ and 90% *asymmetric* confidence interval of the fit, which is determined by a bootstrapping method and takes into account the limits and uncertainties of the measurements. We will see that including the uncertainties of this relation lowers the predicted f_{esc} at a given redshift. The blue region in Figure 2 shows $f_{esc} > 10\%$, i.e., the value that must be reached by $z \sim 6$ such that galaxies can dominate reionization given our current knowledge. We see that these values are reached at [O III]/[O II] $\sim$ 4–7, corresponding to $z \gtrsim 6.5$ for average galaxies at $\log(M/M_\odot) \sim 9.0$ (Figure 1). Finally, we note that the derivation of f_{esc} itself depends on model assumptions. Specifically, the inclusion of a binary stellar population, suggested to be more common at high redshifts (Stanway et al. 2014; Steidel et al. 2016), could lower the derived f_{esc} values.

2.4. Redshift Evolution and Mass Dependence of f_{esc}

Using the redshift evolution of [O III]/[O II] inferred from SDSS galaxies (left panel of Figure 1) and the empirical relation between [O III]/[O II] and f_{esc} (Equation (2), Figure 2), we can now predict f_{esc} as a function of redshift with the given uncertainties. For this end, we use a Monte Carlo sampling approach, taking into account the scatter in the [O III]/[O II] versus redshift relation and the uncertainties/limits in the [O III]/[O II] versus f_{esc} correlation. In detail, we sample 5000 galaxies for each redshift bin and draw [O III]/[O II] ratios to reproduce the observed distribution at a given redshift. For each of these galaxies we then draw f_{esc} from the corresponding [O III]/[O II] ratio, a distribution that we approximate with a skewed Gaussian to take into account its asymmetric uncertainties.

The left panel of Figure 3 shows the final distribution of $f_{esc}(z)$ for different stellar mass bins. The dashed lines include *only* the physical scatter in the [O III]/[O II] versus redshift relation from our LHAs. The solid lines include the physical scatter *and* the uncertainty in the modeling of the [O III]/[O II] versus f_{esc} relation. This in general *lowers* the predicted f_{esc} values (indicated by the arrows), and better constraints on the correlation between [O III]/[O II] and f_{esc} are therefore crucial for a more detailed analysis. We also show the 1σ (90%) confidence interval of the prediction as a dark (light) gray band for the stellar mass range $8.5 < \log(M/M_\odot) < 9.5$

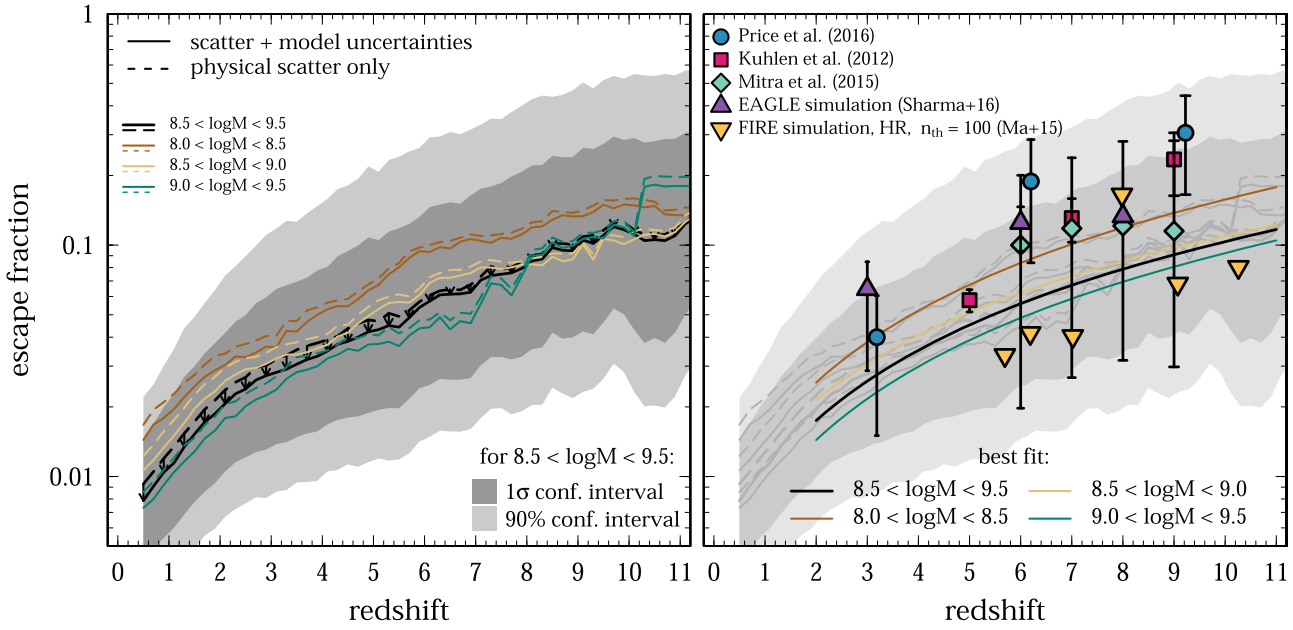

Figure 3. Redshift evolution of f_{esc} inferred from our LHAs. Left: the thick, black solid line shows the prediction for galaxies with $8.5 < \log(M/M_\odot) < 9.5$ together with 1σ (dark gray) and 90% (light gray) confidence intervals, including observed physical scatter in the [O III]/[O II] vs. redshift relation and uncertainties in the [O III]/[O II] vs. f_{esc} fit. The dashed black line shows the prediction including *only* observational scatter (assuming no uncertainty in [O III]/[O II] vs. f_{esc}). The colored solid and dashed lines show the same for $8.0 < \log(M/M_\odot) < 8.5$ (brown), $8.5 < \log(M/M_\odot) < 9.0$ (beige), and $9.0 < \log(M/M_\odot) < 9.5$ (green). Right: comparison of our predicted $f_{esc}(z)$ with model reconstructions (Kuhlen & Faucher-Giguère 2012; Mitra et al. 2015; Price et al. 2016) and simulations (Ma et al. 2015; Sharma et al. 2016) from the literature. The colored lines show the best fits to our predictions parameterized by $f_{esc}(z > 2) = f_{esc,0}((1+z)/3)^\alpha$ for $2 < z < 8$ (see Table 1).

but omit it for the other masses for the sake of clarity. Due to the 10%–15% higher [O III]/[O II] ratios for ∼0.5 dex lower stellar masses (see also Masters et al. 2016), f_{esc} shows a *negative* correlation with stellar mass. In general, f_{esc} is about 50% higher per 0.5 dex smaller stellar mass in the range $8.0 < \log(M/M_\odot) < 9.5$ at $z \sim 6$. From the predicted [O III]/[O II] ratios of local galaxies and the empirical relation between [O III]/[O II] and f_{esc}, we infer $f_{esc} = 5.7^{+8.3}_{-3.3}\%$ at $z = 6$ and $f_{esc} = 10.4^{+15.5}_{-6.3}\%$ at $z = 9$ for $8.5 < \log(M/M_\odot) < 9.5$ on average (errors given as 1σ). Statistically, about 30% of the galaxies at $z \sim 6$ show $f_{esc} > 10\%$, while this fraction becomes 50% at $z \sim 9$. We fit $f_{esc} = f_{esc,0}(1+z)^\alpha$ for $2 < z < 8$ with $f_{esc,0} = (2.3 \pm 0.1)\%$ and $\alpha = 1.17 \pm 0.02$ in the same stellar mass range. The best fits for the different stellar mass bins in the same redshift bin are listed in Table 1. The right panel of Figure 3 compares our prediction of $f_{esc}(z)$ with measurements in the literature from simulations (Ma et al. 2015; Sharma et al. 2016) and f_{esc} reconstructions from *Planck*, Lyα, and QSO data (Kuhlen & Faucher-Giguère 2012; Mitra et al. 2015; Price et al. 2016). In general, our predicted f_{esc} values are lower than in other studies, except for the results from the FIRE simulation (Ma et al. 2015). Other simulations including supernova feedback (important in shaping the ISM and f_{esc}) suggest very similar results for f_{esc} in the range 10%–20% at $z \sim 9$ for our lowest stellar mass bin (Kimm & Cen 2014; Cen & Kimm 2015). All in all, our lowest stellar mass bin is consistent within 1σ with the literature.

It has to be kept in mind that there is a strong dependence of f_{esc} on stellar mass as described above. Simulations suggest a close correlation between mass of the dark matter halo or virial mass and the LyC escape fraction in relative agreement with the trends we find (e.g., Wise & Cen 2009; Razoumov & Sommer-Larsen 2010; Kimm & Cen 2014). Furthermore, a negative correlation is found between Lyα escape fraction and stellar mass (Oyarzún et al. 2016), which suggests a negative correlation between f_{esc} and stellar mass via the close correlation between and LyC escape fraction (Dijkstra & Gronke 2016).

Table 1
Fit to Predicted $f_{esc}(z)$ for Different Stellar Mass Bins

Stellar Mass	$f_{esc,0}$ (%)	α
$8.5 < \log(M/M_\odot) < 9.5$	$1.7^{+0.1}_{-0.2}$	$1.37^{+0.11}_{-0.10}$
$8.0 < \log(M/M_\odot) < 8.5$	$2.5^{+0.2}_{-0.2}$	$1.40^{+0.13}_{-0.10}$
$8.5 < \log(M/M_\odot) < 9.0$	$2.1^{+0.2}_{-0.2}$	$1.26^{+0.11}_{-0.10}$
$9.0 < \log(M/M_\odot) < 9.5$	$1.4^{+0.4}_{-0.3}$	$1.43^{+0.29}_{-0.41}$

Note. Analytical expression: $f_{esc}(z) = f_{esc,0}((1+z)/3)^\alpha$. The fit is performed for $2 < z < 8$.

3. CAN GALAXIES REIONIZE THE UNIVERSE?

We use the LHAs to predict $f_{esc}(z)$ and find $\langle f_{esc} \rangle \sim 6\%$ at $z = 6$ and $\langle f_{esc} \rangle \sim 10\%$ at $z = 9$ for the stellar mass range $8.5 < \log(M/M_\odot) < 9.5$. This prediction comes with a substantial physical scatter (due to the scatter in the [O III]/[O II] ratios at a given redshift) and uncertainty stemming from the poorly constrained [O III]/[O II] versus f_{esc} relation. Statistically, ∼30% of the galaxies show $f_{esc} > 10\%$ by $z = 6$ for $8.5 < \log(M/M_\odot) < 9.5$; however, there is a stellar mass dependence that increases f_{esc} by roughly 50% per 0.5 dex decrease in stellar mass (see Figure 3).

Is this enough for galaxies alone to reionize the universe? The recent study by Price et al. (2016) reconstructs $f_{esc}(z)$ needed for reionization from the latest *Planck* data and finds 2–3 times higher f_{esc} values at $z > 6$ compared to our

predictions. Their findings are just consistent (within 1σ) with our observationally based predictions for f_{esc} for the smallest stellar mass bin ($8.0 < \log(M/M_\odot) < 8.5$). This suggests that the commonly found galaxies at high redshifts with $\log(M/M_\odot) \sim 9.0$ are not sufficient to ionize the early universe; instead the ionization is mostly driven by low-mass, low-luminosity galaxies at $\log(M/M_\odot) \sim 8.0$.

In the following, we want to investigate the above question in more detail and derive two important quantities: $Q_{\rm H\,II}(z)$ (the volume fraction of ionized hydrogen) and $\tau_{\rm el}(z)$ (the integrated electron scattering optical depth). To achieve this end, several assumption have to be made. First, the faint-end cutoff of the UV LF ($M_{\rm UV,lim}$) determines the number of faint galaxies that are available for ionization (similar to the stellar mass function: recall that f_{esc} is anticorrelated with stellar mass). High-redshift galaxies lensed by foreground low-redshift galaxy clusters allow us to probe the UV LF to very faint magnitudes of $M_{\rm UV} \sim -12$ at $z = 6$–8 and have shown no indication of a turnover (Alavi et al. 2014; Livermore et al. 2016). It is therefore safe to assume a value of $-13 < M_{\rm UV,lim} < -10$. Furthermore, the production efficiency of Lyman continuum photons ($\xi_{\rm ion}$) and the clumping factor (C) need to be known. The former is measured observationally and is found to be $\log(\xi_{\rm ion}/[\rm Hz\ erg^{-1}]) = 25.4 \pm 0.1$ for a wide range of galaxy properties at $z \sim 5$ (Bouwens et al. 2015c). The clumping factor $C = \langle n_{\rm H}^2\rangle/\bar{n}_{\rm H}^2$ is proportional to the recombination rate of hydrogen[6] and thus the net production rate of ions. It is commonly constrained from simulations to be between 2 and 5, and we assume $\langle C\rangle = 3$ (e.g., Finlator et al. 2012). Other reasonable values of C have little impact on the following results.

With the relatively good constraints on $\xi_{\rm ion}$ and C and our empirical prediction of $f_{esc}(z)$ we can now derive $Q_{\rm H\,II}(z)$ and $\tau_{\rm el}(z)$ using the following set of basic equations:

$$\tau_{\rm el}(z) = c\,\langle n_{\rm H}\rangle\,\sigma_{\rm T}\int_0^z f_{\rm e}\,Q_{\rm H\,II}(z')H^{-1}(z')(1+z')^2dz' \quad (3)$$

$$\dot{Q}_{\rm H\,II} = \frac{\dot{n}_{\rm ion}}{\langle n_{\rm H}\rangle} - \frac{Q_{\rm H\,II}}{t_{\rm rec}} \quad (4)$$

$$\dot{n}_{\rm ion} = f_{\rm esc}\,\xi_{\rm ion}\,\rho_{\rm uv} \quad (5)$$

$$t_{\rm rec} = [C\ \alpha_B(T)(1 + Y_p/4X_p)\langle n_{\rm H}\rangle(1+z)^3]^{-1} \quad (6)$$

$$\alpha_B = 2.6\times10^{-13}\left(\frac{T}{10^4\ \rm K}\right)^{-0.76}\ \rm cm^3\ s^{-1} \quad (7)$$

$$\langle n_{\rm H}\rangle = 1.67\times10^{-7}\left(\frac{\Omega_b h^2}{0.02}\right)\left(\frac{X_p}{0.75}\right)\rm cm^{-3} \quad (8)$$

where $t_{\rm rec}$ is the hydrogen recombination time with α_B the case-B recombination coefficient. We assume $X_p = 0.75$ for the hydrogen mass fraction (e.g., Hou et al. 2011), the helium mass fraction is given as $Y_p = 1 - X_p$ (Kuhlen & Faucher-Giguère 2012), and the fraction of free electrons as $f_e = 1 + Y_p/2X_p$ at $z \leqslant 4$ and $f_e = 1 + Y_p/4X_p$ at $z > 4$. Furthermore, we use a baryon density $\Omega_b = 0.04$, the Thompson scattering cross section $\sigma_{\rm T} = 6.653\times10^{-25}\,\rm cm^2$, and an IGM temperature $T = 20{,}000$ K. We assume $C = 3$ and $\log(\xi_{\rm ion}) = 25.4$ and 25.6. For the integrated UV luminosity density, $\rho_{\rm uv}$, we use $M_{\rm UV,lim} = -13$ and -10 and the UV LFs of Mason et al. (2015).

With our observationally driven prediction of $f_{esc}(z)$ and our reasonable assumptions for C and $\xi_{\rm ion}$, we can now investigate whether galaxies can reionize the universe by $z \sim 6$. The left panels of Figure 4 show $Q_{\rm H\,II}(z)$ for $M_{\rm UV,lim} = -13$ (top) and -10 (bottom). The 1σ and 90% confidence intervals from our f_{esc} predictions are given for $\log(\xi_{\rm ion}) = 25.4$ and $8.5 < \log(M/M_\odot) < 9.5$. We also show $\log(\xi_{\rm ion}) = 25.6$ as a dashed line for reference. The population-averaged ($8.5 < \log(M/M_\odot) < 9.5$) results are shown in black together with other stellar mass bins with colors as in Figure 3. The right panels of Figure 4 show $\tau_{\rm el}(z)$ with the same color coding and assumptions. We find that galaxies with $\log(M/M_\odot) \sim 9.0$ are capable of ionizing the IGM by $z_{\rm ion} = 5.3^{-1.8}_{+2.4}$ and yield $\tau_{\rm el} \sim 0.05$ with the combination $(M_{\rm UV,lim}, \log\xi_{\rm ion}) = (-13, 25.4)$. Note that this is a population-averaged quantity and single galaxies may show very different escape fractions and therefore contribute to a non-isotropic reionization of the universe. In particular, due to the negative correlation between [O III]/[O II] and stellar mass, a population of low-mass galaxies ($\log(M/M_\odot) \sim 8.0$–8.5) will reionize the universe slightly earlier ($\Delta z \sim 0.5$, so roughly at $z \sim 6$). These findings are in good agreement with measurements of Lyα forest transmission, quasar absorption, and gamma-ray bursts (e.g., Fan et al. 2006; Totani et al. 2006; Bolton & Haehnelt 2007a; Faucher-Giguère et al. 2008; McQuinn et al. 2008; Carilli et al. 2010; Bolton et al. 2011; McGreer et al. 2011; Mortlock et al. 2011; Schroeder et al. 2013) as well as the constraint from *Planck* on the electron scattering optical depth (upper right panel of Figure 4). The combination $(M_{\rm UV,lim}, \log\xi_{\rm ion}) = (-10, 25.4)$ yields $z_{\rm ion} = 6.9^{-3.1}_{+3.5}$, which is also in agreement within uncertainties with the complementary observational constraints, but it overshoots the constraints on $\tau_{\rm el}$ by *Planck*; this leads to too early a reionization. This analysis also depends on the assumed value for $\xi_{\rm ion}$ (see dashed line in Figure 4 showing $\log(\xi_{\rm ion}) = 25.6$); in particular, higher $\xi_{\rm ion}$ have the same effect as a lower stellar mass and lead to an earlier reionization. Several recent studies have suggested that the inclusion of binary stars in the stellar population models may result in higher $\xi_{\rm ion}$ than the current canonical value of $\log(\xi_{\rm ion}) \sim 25.5$ (Stanway et al. 2016; Wilkins et al. 2016). In fact, binary models are expected to be more suitable at high redshifts because of the low-metallicity environments and young stellar populations (Ma et al. 2016; Steidel et al. 2016; Wilkins et al. 2016). If binary populations were prevalent at high redshifts, this would lower the f_{esc} necessary for galaxies to keep the universe ionized at $z < 9$ to modest values of 4%–24%, comparable to our estimates (e.g., Stanway et al. 2016).

Finally, there are not many constraints on the dependence of $\xi_{\rm ion}$ on other galaxy properties. However, Bouwens et al. (2015c) see a weak *negative* trend between the UV continuum slope (β) and $\xi_{\rm ion}$ in their data at $3.8 < z < 5.0$. Assuming a *positive* correlation between stellar mass and β (i.e., more massive galaxies having shallower slopes and likely more dust, e.g., Finkelstein et al. 2012; Bouwens et al. 2014), this would suggest a *smaller* $\xi_{\rm ion}$ for more massive galaxies. These trends thus suggest that less massive galaxies might be even more efficient in ionizing, or, vice versa, more massive galaxies less so.

[6] The recombination rate is proportional to the hydrogen density squared.

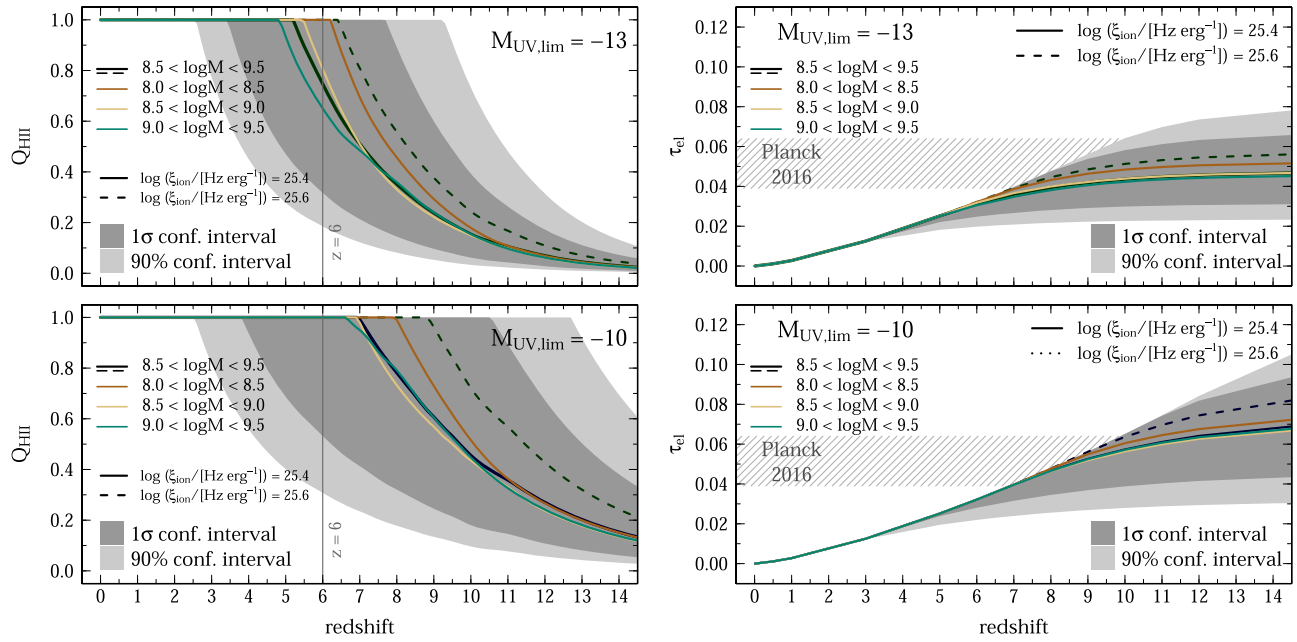

Figure 4. Left: volume fraction of ionized hydrogen as a function of redshift assuming $\log(\xi_{\rm ion}) = 25.4$ for $M_{\rm UV,lim} = -13$ (top) and $M_{\rm UV,lim} = -10$ (bottom) with 1σ and 90% confidence intervals (for $8.5 < \log(M/M_\odot) < 9.5$ only). The different stellar mass bins are indicated with colors. The thin line marks $z < 6$, when the universe is observed to be fully ionized. We also show $\log(\xi_{\rm ion}) = 25.6$ for $8.5 < \log(M/M_\odot) < 9.5$ as a dashed line for reference. Right: electron scattering optical depth integrated up to different redshifts for $M_{\rm UV,lim} = -13$ (top) and $M_{\rm UV,lim} = -10$ (bottom) with 1σ and 90% confidence intervals (for $8.5 < \log(M/M_\odot) < 9.5$ only). The different stellar mass bins are indicated with colors. The gray hatched band marks the recent constraints from *Planck*. We also show $\log(\xi_{\rm ion}) = 25.6$ for $8.5 < \log(M/M_\odot) < 9.5$ as a dashed line. All in all, we find that our observationally based prediction of $f_{\rm esc}$ is just enough for galaxies to reionize the universe by $z \sim 5.3$. Lower-mass galaxies are predicted to reionize the universe by $\Delta z \sim 0.5$ earlier.

4. CONCLUSIONS

We use empirical trends seen in local galaxies to predict emission line ratios and Lyman continuum escape fractions at high redshifts. For this end, we combine the positive correlation of the [O III]/[O II] line ratio and $f_{\rm esc}$ based on low-redshift galaxies with the predicted [O III]/[O II] ratios at high redshift from LHAs. We find increasing [O III]/[O II] line ratios with increasing redshifts, reaching values of [O III]/[O II] $\sim$ 3–4 commonly by $z = 6$, which translates into $f_{\rm esc} > 6\%$ on average at $z > 6$ for galaxies with $\log(M/M_\odot) \sim 9.0$. Statistically, including uncertainties and scatter, roughly 30% of galaxies at $z = 6$ show $f_{\rm esc} > 10\%$, and this fraction increases to 50% at $z = 9$. This first observationally based prediction of $f_{\rm esc}$ suggests that its values for high-redshift galaxies are substantially higher than the currently low $f_{\rm esc}$ limits measured in low-z galaxies, and thus hints toward a strong redshift evolution of $f_{\rm esc}$. However, we also find a strong stellar mass dependence of $f_{\rm esc}$, driven by the stellar mass dependence of the [O III]/[O II] ratio. In particular, a decrease by 0.5 dex in stellar mass results in an *increase* in $f_{\rm esc}$ of 50%. Note that this is in agreement with the dark matter halo dependence of $f_{\rm esc}$ predicted by various simulations. If true, the stellar mass function and its evolution with redshift—which is likely coupled with the rest-UV LF—is an important ingredient for assessing the importance of galaxies in the EoR. With our observationally based prediction for the population-averaged $f_{\rm esc}(z)$ (thus fixing an important, previously unknown variable) and reasonable assumptions for C and $\xi_{\rm ion}$ we find that galaxies at $\log(M/M_\odot) \sim 9.0$ release a sufficiently large number of ionizing photons to reionize the universe by $z_{\rm ion} = 5.3^{-1.8}_{+2.4}$ for $M_{\rm UV,lim} = -13$ and by $z_{\rm ion} = 6.9^{-3.1}_{+3.5}$ for $M_{\rm UV,lim} = -10$. Galaxies of lower masses are able to reionize the universe by $\Delta z \sim 0.5$ earlier.

This work should be understood as the beginning of a more detailed study of $f_{\rm esc}$ during the EoR. Until now, this has been hampered by the large uncertainties in the [O III]/[O II] versus $f_{\rm esc}$ relation. Furthermore, the link between LHA and actual very high-redshift galaxies needs to be explored in more detail. Future spectroscopic observations by the *Hubble Space Telescope* will enhance the sample sizes of galaxies with LyC detection and will add to a better understanding of the link between [O III]/[O II] and $f_{\rm esc}$. Furthermore, *WFIRST* and *JWST* will ultimately measure [O III] and [O II] in high-redshift galaxies and thus verify the link between local galaxies and the first galaxies formed.

The author would like to thank Dan Masters, Peter Capak, Janice Lee, and Kirsten Larson for valuable discussions that improved this manuscript. Furthermore, the author would like to thank the anonymous referee for very useful feedback. A.F. acknowledges support from the Swiss National Science Foundation.

REFERENCES

Alam, S., Albareti, F. D., Allende Prieto, C., et al. 2015, ApJS, 219, 12
Alavi, A., Siana, B., Richard, J., et al. 2014, ApJ, 780, 143
Bian, F., Kewley, L. J., Dopita, M. A., & Juneau, S. 2016, ApJ, 822, 62
Bolton, J. S., & Haehnelt, M. G. 2007a, MNRAS, 381, L35
Bolton, J. S., & Haehnelt, M. G. 2007b, MNRAS, 382, 325
Bolton, J. S., Haehnelt, M. G., Warren, S. J., et al. 2011, MNRAS, 416, L70
Borthakur, S., Heckman, T. M., Leitherer, C., & Overzier, R. A. 2014, Sci, 346, 216
Bouwens, R. J., Illingworth, G. D., Oesch, P. A., et al. 2014, ApJ, 793, 115
Bouwens, R. J., Illingworth, G. D., Oesch, P. A., et al. 2015a, ApJ, 811, 140
Bouwens, R. J., Illingworth, G. D., Oesch, P. A., et al. 2015b, ApJ, 803, 34

Bouwens, R. J., Smit, R., Labbe, I., et al. 2015c, arXiv:1511.08504
Cardamone, C., Schawinski, K., Sarzi, M., et al. 2009, MNRAS, 399, 1191
Carilli, C. L., Wang, R., Fan, X., et al. 2010, ApJ, 714, 834
Cen, R., & Kimm, T. 2015, ApJL, 801, L25
Chabrier, G. 2003, PASP, 115, 763
Colbert, J. W., Teplitz, H., Atek, H., et al. 2013, ApJ, 779, 34
Cooke, J., Ryan-Weber, E. V., Garel, T., & Díaz, C. G. 2014, MNRAS, 441, 837
de Barros, S., Vanzella, E., Amorín, R., et al. 2016, A&A, 585, A51
de los Reyes, M. A., Ly, C., Lee, J. C., et al. 2015, AJ, 149, 79
Dijkstra, M., & Gronke, M. 2016, arXiv:1604.08208
Erb, D. K., Pettini, M., Steidel, C. C., et al. 2016, arXiv:1605.04919
Erb, D. K., Steidel, C. C., Shapley, A. E., et al. 2006, ApJ, 647, 128
Faisst, A. L., Capak, P., Carollo, C. M., Scarlata, C., & Scoville, N. 2014, ApJ, 788, 87
Faisst, A. L., Capak, P., Hsieh, B. C., et al. 2016a, ApJ, 821, 122
Faisst, A. L., Capak, P. L., Davidzon, I., et al. 2016b, ApJ, 822, 29
Fan, X., Strauss, M. A., Becker, R. H., et al. 2006, AJ, 132, 117
Faucher-Giguère, C.-A., Prochaska, J. X., Lidz, A., Hernquist, L., & Zaldarriaga, M. 2008, ApJ, 681, 831
Finkelstein, S. L., Papovich, C., Salmon, B., et al. 2012, ApJ, 756, 164
Finlator, K., Oh, S. P., Özel, F., & Davé, R. 2012, MNRAS, 427, 2464
Förster Schreiber, N. M., Shapley, A. E., Erb, D. K., et al. 2011, ApJ, 731, 65
Gnedin, N. Y., Kravtsov, A. V., & Chen, H.-W. 2008, ApJ, 672, 765
Grazian, A., Giallongo, E., Gerbasi, R., et al. 2016, A&A, 585, A48
Greis, S. M. L., Stanway, E. R., Davies, L. J. M., & Levan, A. J. 2016, MNRAS, 459, 2591
Guaita, L., Pentericci, L., Grazian, A., et al. 2016, A&A, 587, A133
Hayashi, M., Ly, C., Shimasaku, K., et al. 2015, PASJ, 67, 80
Hemmati, S., Mobasher, B., Darvish, B., et al. 2015, ApJ, 814, 46
Hou, L. G., Han, J. L., Kong, M. Z., & Wu, X.-B. 2011, ApJ, 732, 72
Hu, E. M., Cowie, L. L., Kakazu, Y., & Barger, A. J. 2009, ApJ, 698, 2014
Inoue, A. K., Iwata, I., & Deharveng, J.-M. 2006, MNRAS, 371, L1
Inoue, A. K., Shimizu, I., Iwata, I., & Tanaka, M. 2014, MNRAS, 442, 1805
Izotov, Y. I., Orlitová, I., Schaerer, D., et al. 2016a, Natur, 529, 178
Izotov, Y. I., Schaerer, D., Thuan, T. X., et al. 2016b, MNRAS, 461, 3683
Khaire, V., Srianand, R., Choudhury, T. R., & Gaikwad, P. 2016, MNRAS, 457, 4051
Khostovan, A. A., Sobral, D., Mobasher, B., et al. 2016, arXiv:1604.02456
Kimm, T., & Cen, R. 2014, ApJ, 788, 121
Kuhlen, M., & Faucher-Giguère, C.-A. 2012, MNRAS, 423, 862
Le Fèvre, O., Cassata, P., Cucciati, O., et al. 2013, A&A, 559, A14
Leitet, E., Bergvall, N., Hayes, M., Linné, S., & Zackrisson, E. 2013, A&A, 553, A106
Leitherer, C., Hernandez, S., Lee, J. C., & Oey, M. S. 2016, ApJ, 823, 64
Livermore, R. C., Finkelstein, S. L., & Lotz, J. M. 2016, arXiv:1604.06799
Ma, X., Hopkins, P. F., Kasen, D., et al. 2016, MNRAS, 459, 3614
Ma, X., Kasen, D., Hopkins, P. F., et al. 2015, MNRAS, 453, 960
Madau, P. 1995, ApJ, 441, 18
Madau, P., & Haardt, F. 2015, ApJL, 813, L8
Maiolino, R., Nagao, T., Grazian, A., et al. 2008, A&A, 488, 463
Mason, C. A., Trenti, M., & Treu, T. 2015, ApJ, 813, 21
Masters, D., Capak, P., Salvato, M., et al. 2012, ApJ, 755, 169
Masters, D., Faisst, A., & Capak, P. 2016, ApJ, 828, 18
Matthee, J. J. A., Sobral, D., Swinbank, A. M., et al. 2014, MNRAS, 440, 2375
McGreer, I. D., Mesinger, A., & Fan, X. 2011, MNRAS, 415, 3237
McQuinn, M., Lidz, A., Zaldarriaga, M., Hernquist, L., & Dutta, S. 2008, MNRAS, 388, 1101
Mitra, S., Choudhury, T. R., & Ferrara, A. 2015, MNRAS, 454, L76
Mortlock, D. J., Warren, S. J., Venemans, B. P., et al. 2011, Natur, 474, 616
Nakajima, K., & Ouchi, M. 2014, MNRAS, 442, 900
Oesch, P. A., Bouwens, R. J., Illingworth, G. D., et al. 2014, ApJ, 786, 108
Ono, Y., Ouchi, M., Mobasher, B., et al. 2012, ApJ, 744, 83
Oyarzún, G. A., Blanc, G. A., González, V., et al. 2016, ApJL, 821, L14
Palanque-Delabrouille, N., Magneville, C., Yèche, C., et al. 2013, A&A, 551, A29
Planck Collaboration, Aghanim, N., Ashdown, M., et al. 2016, arXiv:1605.02985
Price, L. C., Trac, H., & Cen, R. 2016, arXiv:1605.03970
Razoumov, A. O., & Sommer-Larsen, J. 2010, ApJ, 710, 1239
Rigby, J. R., Wuyts, E., Gladders, M. D., Sharon, K., & Becker, G. D. 2011, ApJ, 732, 59
Roberts-Borsani, G. W., Bouwens, R. J., Oesch, P. A., et al. 2015, ApJ, 823, 143
Robertson, B. E., Ellis, R. S., Furlanetto, S. R., & Dunlop, J. S. 2015, ApJL, 802, L19
Rutkowski, M. J., Scarlata, C., Haardt, F., et al. 2016, ApJ, 819, 81
Sandberg, A., Östlin, G., Melinder, J., Bik, A., & Guaita, L. 2015, ApJL, 814, L10
Sanders, R. L., Shapley, A. E., Kriek, M., et al. 2016, ApJ, 816, 23
Schenker, M. A., Robertson, B. E., Ellis, R. S., et al. 2013, ApJ, 768, 196
Schroeder, J., Mesinger, A., & Haiman, Z. 2013, MNRAS, 428, 3058
Scoville, N., Aussel, H., Brusa, M., et al. 2007, ApJS, 172, 1
Sharma, M., Theuns, T., Frenk, C., et al. 2016, MNRAS, 458, L94
Siana, B., Shapley, A. E., Kulas, K. R., et al. 2015, ApJ, 804, 17
Silverman, J. D., Kashino, D., Sanders, D., et al. 2015, ApJS, 220, 12
Smith, B. M., Windhorst, R. A., Jansen, R. A., et al. 2016, arXiv:1602.01555
Sobral, D., Matthee, J., Best, P. N., et al. 2015, MNRAS, 451, 2303
Stanway, E. R., Eldridge, J. J., & Becker, G. D. 2016, MNRAS, 456, 485
Stanway, E. R., Eldridge, J. J., Greis, S. M. L., et al. 2014, MNRAS, 444, 3466
Stark, D. P., Ellis, R. S., Chiu, K., Ouchi, M., & Bunker, A. 2010, MNRAS, 408, 1628
Steidel, C. C., Pettini, M., & Adelberger, K. L. 2001, ApJ, 546, 665
Steidel, C. C., Rudie, G. C., Strom, A. L., et al. 2014, ApJ, 795, 165
Steidel, C. C., Strom, A. L., Pettini, M., et al. 2016, ApJ, 826, 159
Tacchella, S., Trenti, M., & Carollo, C. M. 2013, ApJL, 768, L37
Totani, T., Kawai, N., Kosugi, G., et al. 2006, PASJ, 58, 485
Vanzella, E., De Barros, S., Cupani, G., et al. 2016a, ApJL, 821, L27
Vanzella, E., de Barros, S., Vasei, K., et al. 2016b, ApJ, 825, 41
Vanzella, E., Giavalisco, M., Inoue, A. K., et al. 2010, ApJ, 725, 1011
Vasei, K., Siana, B., Shapley, A. E., et al. 2016, arXiv:1603.02309
Wilkins, S. M., Feng, Y., Di-Matteo, T., et al. 2016, MNRAS, 458, L6
Wise, J. H., & Cen, R. 2009, ApJ, 693, 984
York, D. G., Adelman, J., Anderson, J. E., Jr., et al. 2000, AJ, 120, 1579